

SUPPLEMENTARY

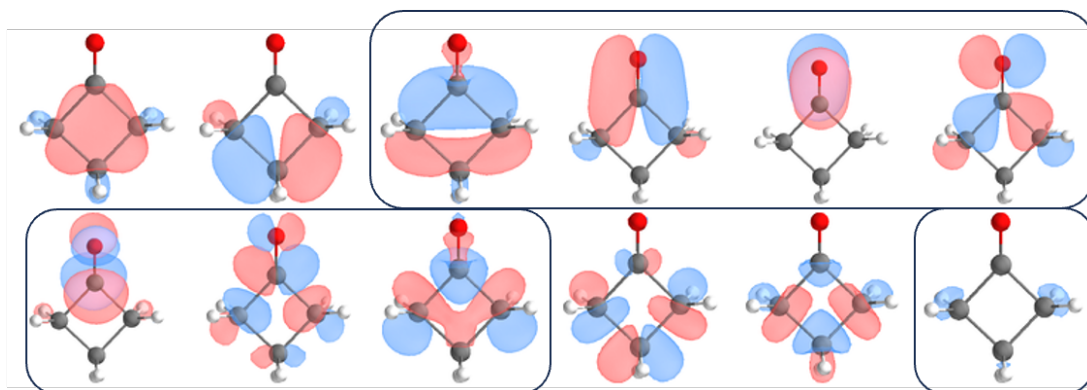


Figure S1: CASSCF [12,12] and CASSCF [8,8] active-spaces utilized in this work

XMS-CASPT2 [12,12]

	6-31G*/8s8p8d	6-31G*/1s1p1d	6-31++G*	Aug-cc-pvdz	Aug-cc-pvtz
¹ NPI*	4.24	4.34	4.32	4.25	4.24
¹ N RYDBERG	6.28	6.36	6.34	6.24	6.50
³ NPI*	4.03	4.02	4.02	3.93	3.92
³ PIPI*	6.28	6.25	6.21	6.21	6.18
³ N RYDBERG	6.16	6.24	6.27	6.10	6.36

Vertical excitation energies in eV on MP2 OPTIMIZED geometry at XMS-CASPT2 level with $|12,12|$ active-space with various basis-sets employing diffuse functions.

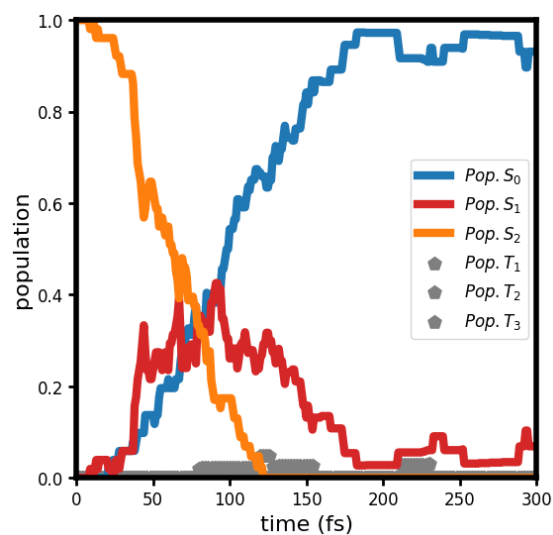


Figure S2: CASSCF $|12,12|$ dynamics. Time dependent population of the three lowest singlet and triplet adiabatic states computed through average occupation numbers in the ensemble of trajectories.

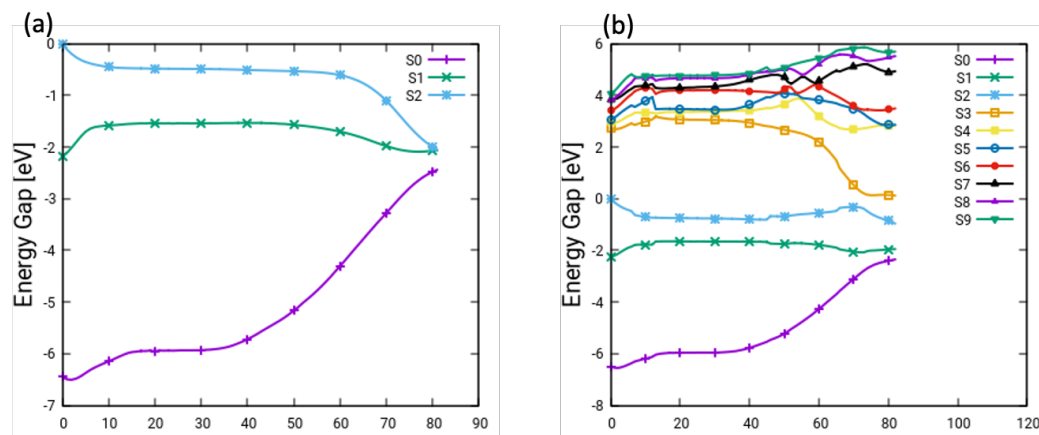


Figure S3: (a) CASSCF $|12,12|$ IRC path. (b) Single points with 10 electronic states computed at $|12,12|$ CASSCF level on CASSCF IRC showing the influence of higher electronic states at Franck-Condon in the IRC

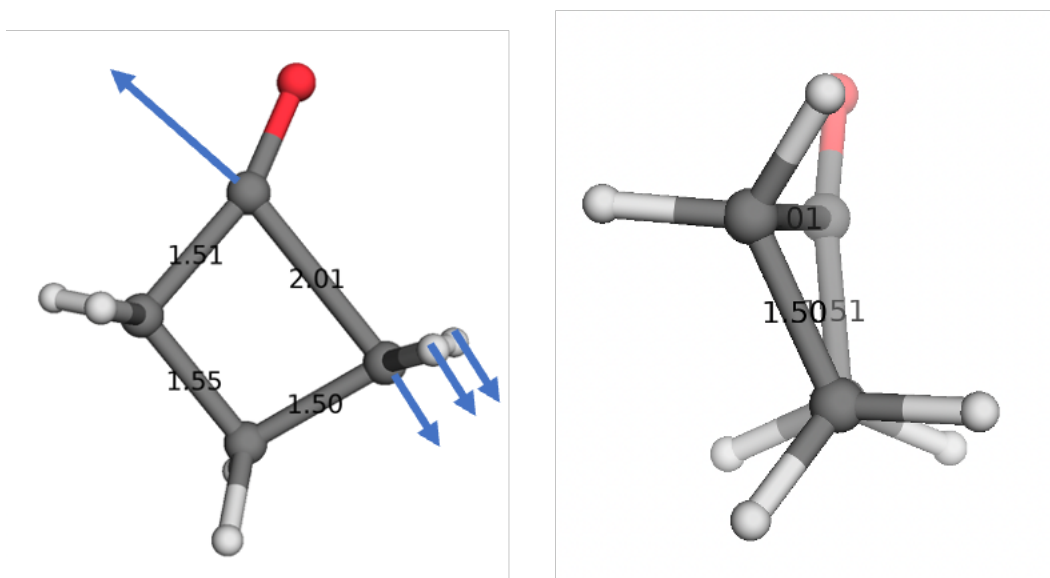


Figure S4: Normal mode corresponding to the negative frequency at 608 cm^{-1} for the Transition-State on the S_2 surface optimized at XMS-CASPT2 level.

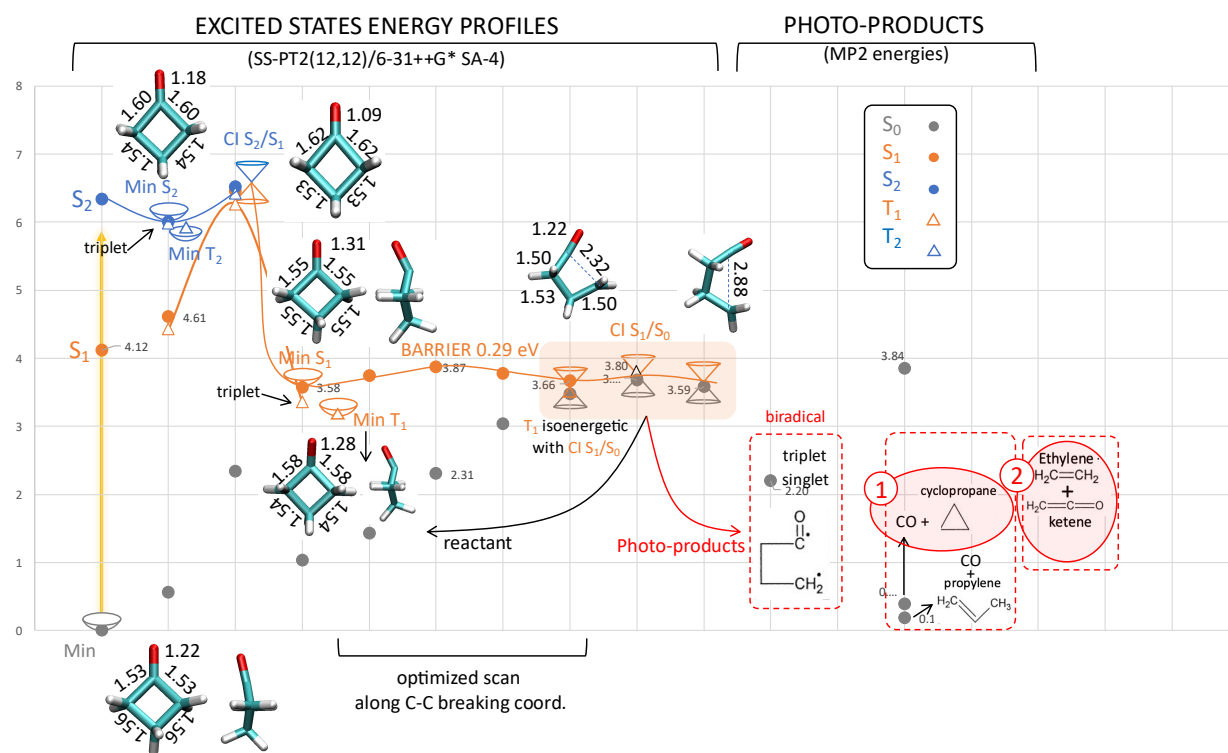


Figure S5: The minor reaction path corresponding to the CI between the $n\pi^*$ and $n \rightarrow (3s)$ Rydberg state

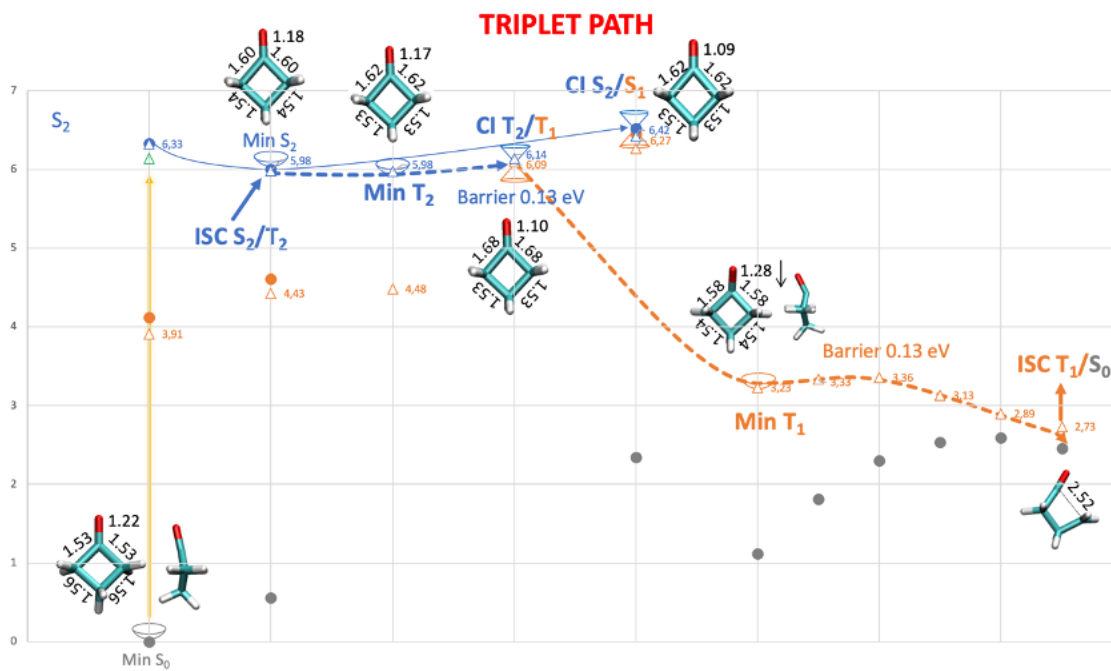


Figure S6: The reaction path in case of population of the T2 state while the dynamics are trapped in the region of S2-minima.

XMS-CASPT2 modified scattering intensity

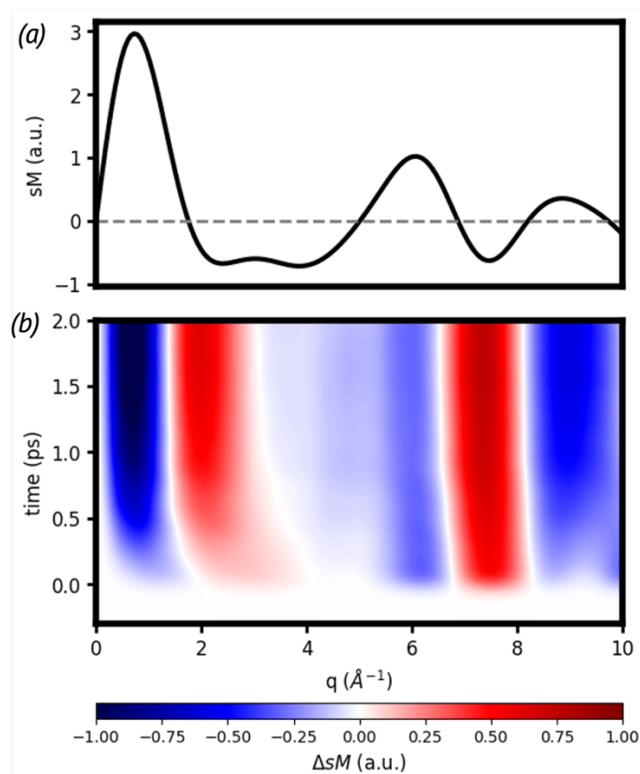


Figure S7 (a) Ground state modified scattering intensity ($sM(q)$) and its time dependent version (b) computed starting from XMS-CASPT2 trajectories. The predicted results have been convoluted with a gaussian function with FWHM of 150 fs mimicking the experimental time resolution.

XMS-CASPT2 UED signals with infinite time resolution

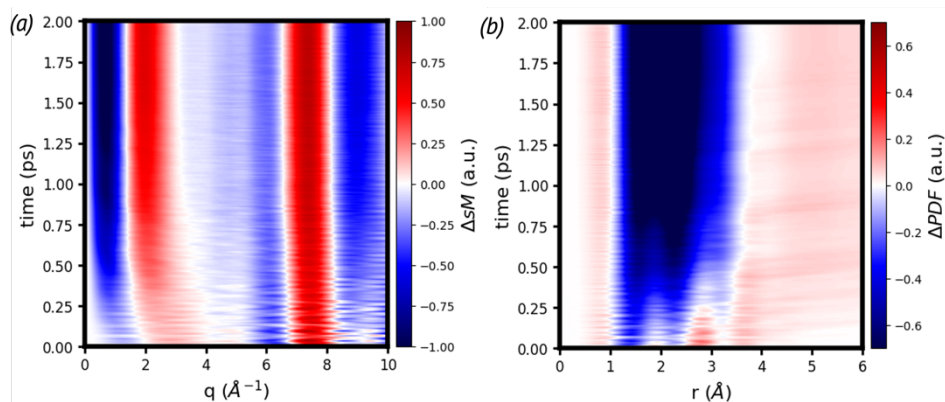


Figure S8. (a) predicted modified scattering intensity $\Delta sM(q)$ and (b) time dependent pair distribution function $\Delta PDF(r)$ computed from XMS-CASPT2 trajectories without accounting for the experimental time resolution.

UED signals from CASSCF trajectories

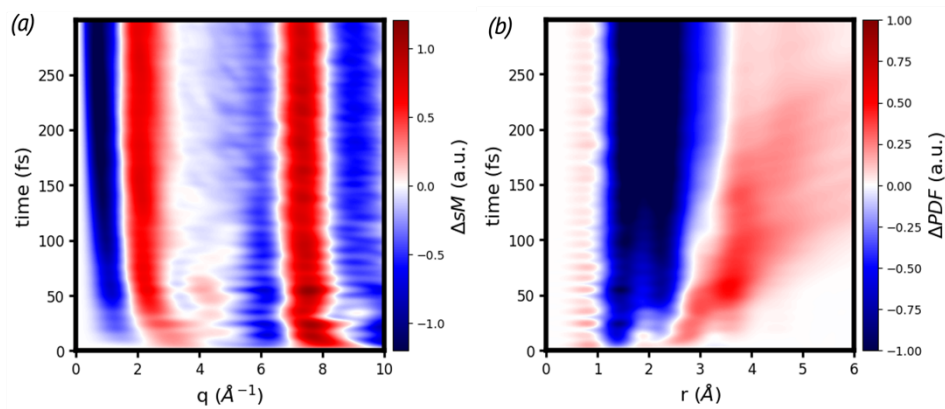


Figure S9. (a) predicted modified scattering intensity and (b) time dependent pair distribution function computed from CASSCF trajectories without accounting for the experimental time resolution.

Comparison between IAM and ab-initio UED simulations

In this section we simulate UED signals from ab-initio electron densities computed for three different CASSCF(12,12) IRC steps (namely: 15,45 and 80) by post processing them as described in [doi.org/10.1063/4.0000043]. These scattering patterns are compared with the signals predicted by the IAM to assess the strength of the individual atom approximation.

Fig. S10 shows that the main differences between IAM and ab-initio signals are observed for momentum transfer values (q) smaller than 5 Angstrom while, for large q values, the two approaches look almost identical. This behavior is expected since at large momentum transfers the main contribution to the UED signal comes from the nuclear scattering (i.e., those electrons that are scattered directly by the nuclei) which is properly captured already in the IAM. The difference between the IAM and ab-initio approach at low momentum is thus originated by the electron-electron and mixed electron-nuclear scattering interactions which are better described when ab-initio electron densities are employed. However, these differences become even less relevant when looking to the Fourier transform of the modified diffraction patterns (i.e., the pair distribution function in the real space) since they do not affect the global behavior of the signal.

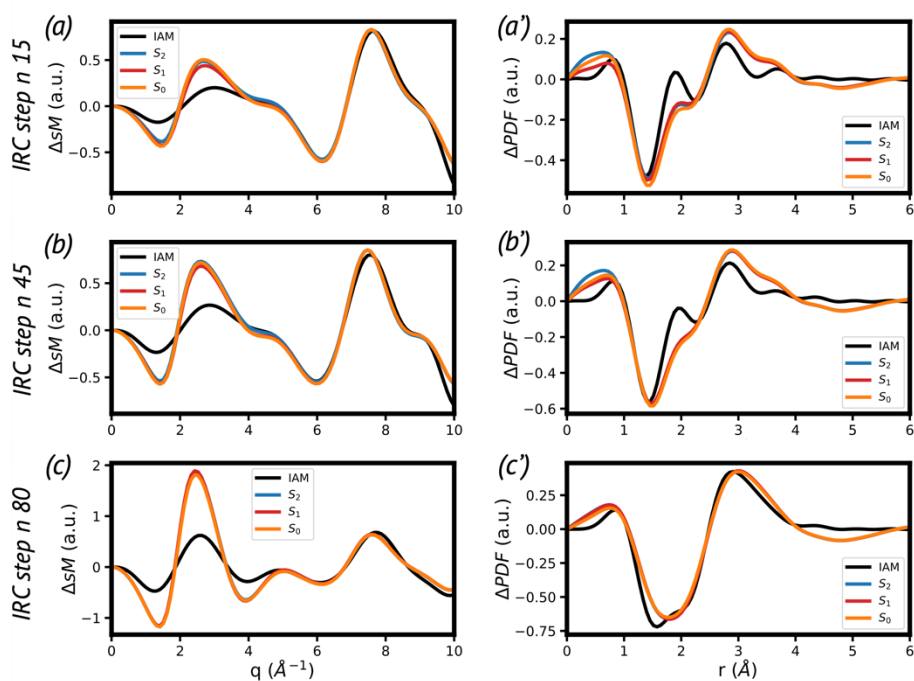


Figure S10. Comparison between the IAM and ab-initio UED simulations performed on some structures of the CASSCF(12,12) IRC path (i.e., step number 15 (a/a'), 45 (b/b') and 80 (c/c') of figure S3-(a)). In particular, a,b, and c compare the modified scattering intensity predicted through IAM with those obtained employing the electron densities of the three main electronic states involved in the ring fragmentation process (S2, S1 and S0). Panels, a',b' and c', analogously, compare the Fourier transform of the modified scattering intensity (i.e., the radial pair distribution function) obtained with the two different approaches.

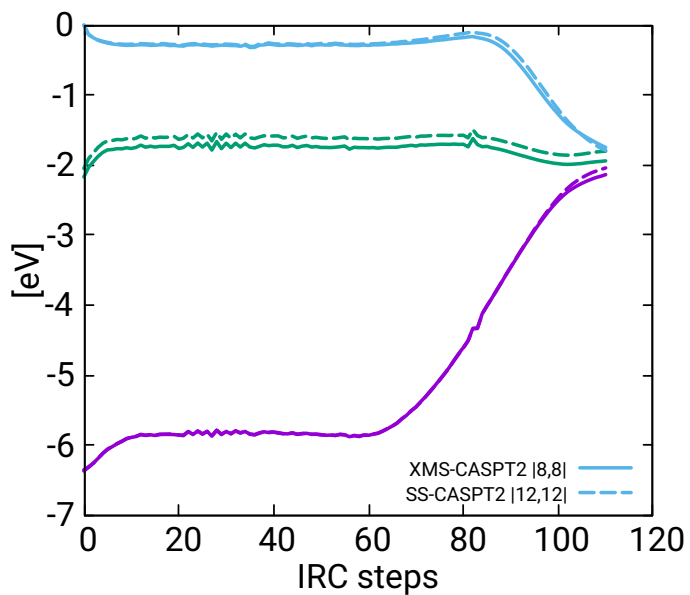
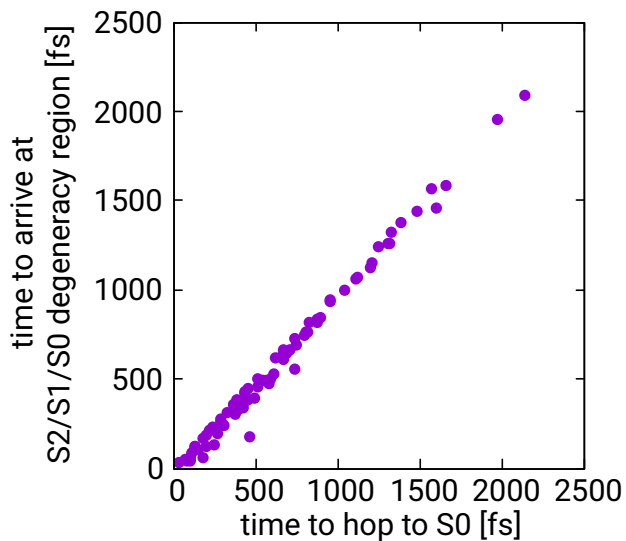


Figure S11: Comparison of the energetic profile of relevant electronic states along major reaction path with two different active-spaces at CASPT2 level.

(a)



(b)

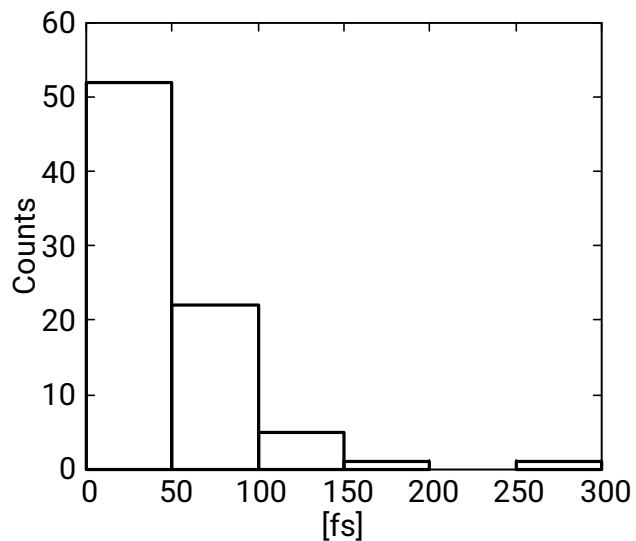


Figure S12: (a) hopping time vs the time to arrive at three-state degeneracy region. (b) Distribution of time spent in three-state degeneracy region

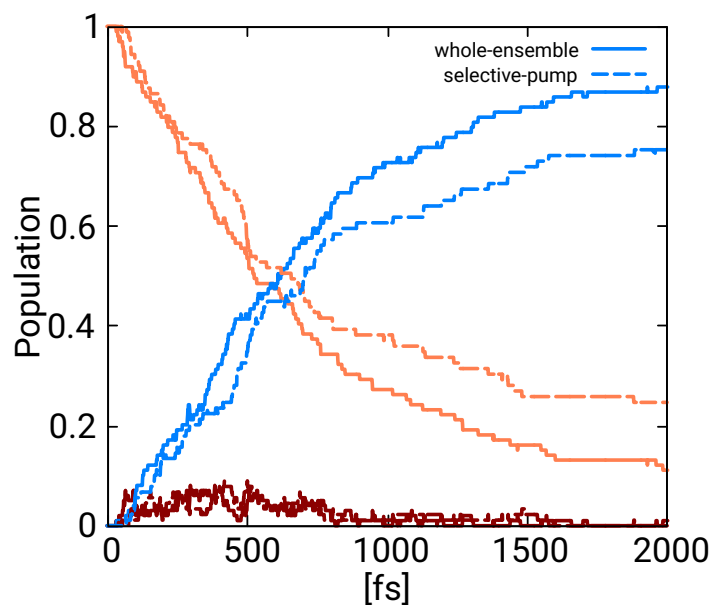


Figure S13: Comparison of non-adiabatic dynamics by selecting geometries with Rydberg excitation lying within 6-6.2 eV (*selective pump*) versus selecting all geometries in Wigner ensemble (*whole-ensemble*). *Whole-ensemble* consists of 100 geometries while *selective-pump* ensemble consists of 89 geometries.

Product	%
CO+cyclopropane	41
Ethene + ketene	39
CO+propylene	4
cyclobutanone	4

Table S2: Quantum yield of photoproducts in selective pump dynamics

Coordinates of critical geometries optimized at CASPT2 level

Min S0

C	-0.387848	-1.104413	0.074740
C	-1.470042	-0.000011	-0.086827
C	-0.387859	1.104436	0.074497
C	0.658865	-0.000001	-0.091599
O	1.849145	-0.000024	-0.351073
H	-0.350727	1.914687	-0.659990
H	-0.353464	1.534715	1.082566
H	-1.914412	-0.000124	-1.085465
H	-2.268719	0.000067	0.658052
H	-0.350707	-1.914823	-0.659570
H	-0.353449	-1.534471	1.082903

Min S2

C	-0.451410	-1.082527	0.004298
C	-1.539687	-0.000004	-0.018125
C	-0.451421	1.082535	0.004060
C	0.732631	0.000012	0.028149
O	1.909024	0.000020	0.052038
H	-0.287637	1.646588	-0.926465
H	-0.325616	1.646289	0.940656
H	-2.132471	-0.000107	-0.932404
H	-2.169413	0.000090	0.871111
H	-0.287620	-1.646783	-0.926103
H	-0.325599	-1.646075	0.941018

Min S1

C	-0.395994	-1.090507	0.013226
C	-1.492874	-0.000011	-0.078396
C	-0.396004	1.090517	0.012987
C	0.642833	-0.000032	-0.371190
O	1.882219	0.000020	0.043657
H	-0.448718	1.946559	-0.665191
H	-0.217598	1.435264	1.040107
H	-1.994444	-0.000119	-1.048358
H	-2.242355	0.000073	0.715734
H	-0.448699	-1.946699	-0.664764
H	-0.217584	-1.435027	1.040422

CI S2S1

C	-0.485643	-1.049046	0.000404
C	-1.597783	-0.000006	-0.035524
C	-0.485654	1.049052	0.000177
C	0.752086	0.000010	0.005383
O	1.839969	0.000018	0.029564
H	-0.220497	1.555676	-0.934188
H	-0.275344	1.514084	0.992646
H	-2.172636	-0.000109	-0.954888
H	-2.187906	0.000090	0.875528
H	-0.220483	-1.555877	-0.933847
H	-0.275327	-1.513855	0.992978

MinT1

C	-0.401276	-1.081174	0.017429
C	-1.498153	0.000186	-0.078168
C	-0.402350	1.081673	0.016937
C	0.661802	-0.000139	-0.413575
O	1.855994	-0.001652	0.058220
H	-0.448083	1.941449	-0.656496
H	-0.203154	1.405244	1.046027
H	-1.989314	-0.000171	-1.053065
H	-2.253714	0.000225	0.709603
H	-0.448027	-1.941311	-0.655424
H	-0.202942	-1.404291	1.046746

Min T2

C	-0.459400	-1.087967	0.004294
C	-1.538945	-0.000004	-0.018246
C	-0.459411	1.087975	0.004055
C	0.741036	0.000012	0.028136
O	1.913925	0.000021	0.051423
H	-0.286478	1.650395	-0.926578
H	-0.324650	1.649786	0.941410
H	-2.133470	-0.000107	-0.931151
H	-2.170730	0.000090	0.869334
H	-0.286462	-1.650591	-0.926215
H	-0.324633	-1.649572	0.941773

